NARROW BANDGAP GaSb AND InGaAsSb/GaSb BASED CELLS FOR MECHANICALLY STACKED TANDEMS AND TPV CONVERTERS

V.P. Khvostikov, V.D. Rumyantsev, O.A. Khvostikova, P.Y. Gazaryan,
S.V. Sorokina, N.S. Potapovich, M.Z. Shvarts, V.M. Andreev
Ioffe Physico-Technical Institute, 26 Polytechnicheskaya, 194021, St. Petersburg, Russia
Tel: +7-812-2475649, Fax: +7-812-2471017, e-mail: vlkhv@scell.ioffe.rssi.ru

ABSTRACT: In this work, LPE growth of GaSb and InGaAsSb and Zn-diffusion techniques were applied for manufacturing the mechanically stacked solar cells and TPV cells. GaSb layers grown by the LPE technique and doped with tellurium were investigated for growth temperatures 520 ^{0}C and 400 ^{0}C. These layers were used for formation of PV cells. The maximum efficiency of 6 % has been achieved for GaSb cells behind GaAs top cell at concentration ratio of 100-200 suns, and 5.2 % behind a top double-junction GaInP/GaInAs cell with GaAs substrate of 250 μm in thickness. Efficiency of 19 % was measured in GaSb TPV cells illuminated by solar powered tungsten emitter.
Keywords: LPE, Tandem, Thermophotovoltaics

1 INTRODUCTION

Photocells based on GaSb and related compounds may be regarded as a basis for at least two photovoltaic applications – the bottom subcells in mechanically stacked solar cells [1-3] and the thermophotovoltaic (TPV) converters [4, 5].

Very often GaSb based cells are formed by simple diffusion technique with use of wafers prepared from bulk material. Obviously, output characteristics of photoconverters depend to a large extent on the initial material quality. Epitaxial layers are characterized by higher purity and morphology perfection compared to the material of a substrate on which they are grown. For example, introduction of an epitaxial *n*-GaSb base layer into the photocell structure gives rise to better reproducibility of device parameters, allows reducing quantity of the residual impurities, as well as lowering down the effect of the intrinsic structural point defects. Also, epitaxial growth of the low resistance contact layers with a high doping level is neccesary to reduce internal ohmic losses in the cells generating high photocurrent.

In this work, high efficient GaSb and InGaAsSb based photovoltaic cells for solar and TPV applications fabricated by means of combination of LPE and Zn-diffusion techniques are investigated. In particular, different kinds of contact structures to *p*- and *n*-type top GaSb layers were studied, PV conversion efficiencies in bottom cells in the case of mechanical stack have been calculated and measured, operation of the developed cells in a solar powered TPV system have been checked.

2 GaSb INGOTS AND EPITAXIAL LAYERS PROPERTIES COMPARISON

Growth of Te-doped GaSb layers was carried out in the hydrogen atmosphere in a horizontal quartz reactor by the liquid phase epitaxy technique with the use of a graphite boat. It was realized from a melt enriched with gallium on the GaSb substrates (100) orientated. Layer thicknesses were varied from 10 to 15 μm at the crystallization temperatures started from 520 ^{0}C, or 400 ^{0}C. The values of concentrations and mobilities of charge carriers were taken from the Hall measurements.

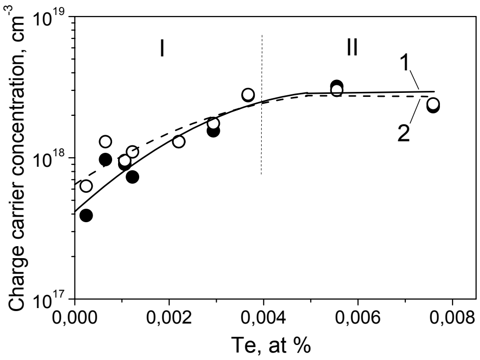

Figure 1: Free electron concentration in *n*-GaSb layers grown by LPE vs. tellurium content in the liquid phase: curve 1 (–●–) - at 300 K, curve 2 (–○–) - at 77 K.

Two regions can be distinguished on the dependencies of charge carrier concentration on tellurium content in liquid phase for GaSb layers grown at 520 ^{0}C (Fig. 1). The first one corresponds to a noticeable rise in the concentration when tellurium content increases up to 0.004 at. %. The second one reflects the fact that further increase in tellurium content up to 0.01 at. % in liquid phase does not result in corresponding increase of carrier concentration.

It is seen from Fig. 2, that the mobility of charge carriers in the epitaxial layers decreases from 4500 cm^2/ V·sec to 2500 cm^2/ V·sec with increasing the concentration from $4\cdot10^{17}$ cm^{-3} to $4\cdot10^{18}$ cm^{-3}. This fact may be explained by the effect of the charge carrier scattering by ionized impurity atoms because at room temperature the majority of impurity atoms are ionized. The epitaxial layers with $n = 5\cdot10^{17}$ cm^{-3} are characterized by mobilities of 4000 cm^2/ V·sec and 8000 cm^2/ V·sec at T = 300 K and T = 77 K, respectively. The layers with tellurium concentration of $n = (3–6)\cdot10^{17}$ см$^{-3}$ were used by us for formation of the photoactive region in PV cells. The heavily doped n^+-layers ($\geq 10^{18}$ см$^{-3}$) were used as back surface layers allowing reduction in ohmic contact resistivity (as low as 10^{-6} Ω·cm^2). Also, such layers can be employed in monolithic tandem cells for formation of tunnel *p-n* junctions. It is clear from Fig. 2 that the epitaxial growth temperature exerts influence on carrier mobility in layers. For instance, the samples grown at

$\sim 400\ ^0C$ are characterized by lower mobilities than those grown at $\sim 520\ ^0C$.

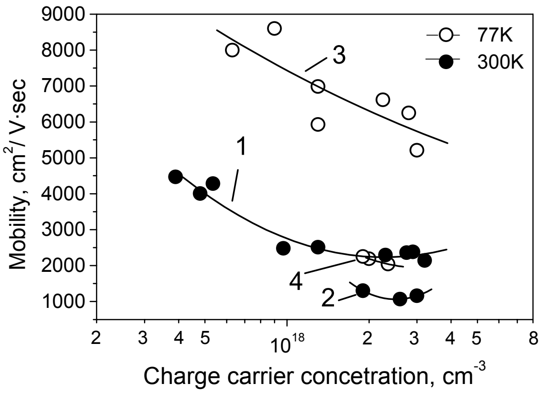

Figure 2: Dependences of the mobility of charge carriers on their concentration in the *n*-GaSb epitaxial layers grown at $\sim 520\ ^0C$ (curves 1, 3) and $\sim 400\ ^0C$ (curves 2, 4).

Figure 3 shows our experimental data concerned with mobility measurements in *n*-GaSb wafers of ingot material grown by the Czochralski technique. As it is seen from Figure, the charge carrier mobility values are significantly lower than in the case of epitaxial material (see Fig. 2) for both 77 K and 300 K at free electron concentration of $5{\cdot}10^{17}$ cm.[3]

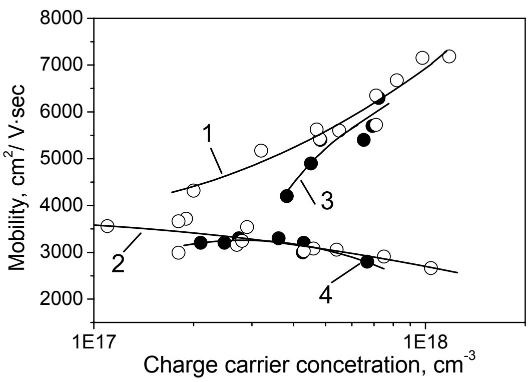

Figure 3: Dependences of the mobility of charge carriers on their concentration in *n*-GaSb wafers from ingots № 93 (–•–) and № 96 (–○–): at T = 300 K (curve 2, 4) and T = 77 K (curve 1, 3).

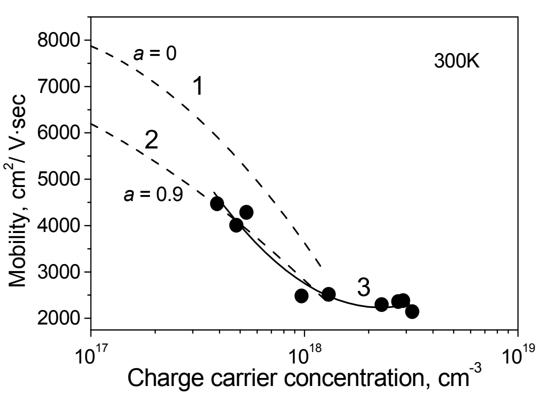

Figure 4: Dependences of the mobility of charge carriers on their concentration in the *n*-GaSb epitaxial layers: 1, 2 - calculations for $a = 0$ and $a = 0.9$ [6,7]; 3 - experiment.

Fig. 4 presents theoretical values of electron mobility in GaSb for compensation ratios of $a = 0$ and $a = 0.9$ (dotted curves 1, 2 [6, 7]). Here $a = N_a / N_d$ (N_A and N_D are the acceptor and donor densities, respectively). In the same figure, our experimental data for epitaxial layers grown at temperature of 520^0C are shown by curve 3. It is seen that experimental data are close to theoretical once for the case of $a = 0.9$ and at growth temperatures higher than $500\ ^0C$.

3 OHMIC CONTACTS TO GaSb

The problem of lowering down the ohmic losses is very important for technology of both concentrator solar cells and thermophotovoltaic converters operating at high intensities of illumination. In this work, different kinds of contacts to *p*- and *n*-type gallium antimonide were studied with the aim to reduce the resistance of the metal-semiconductor contact. The contact resistance values were measured by the transmission line method (TLM) with a radial geometry of contact areas [8].

To form *p-n* junctions in GaSb-based solar cells and TPV converters, the diffusion of Zn from a gas phase was used. Heavy doping of the surface region after the Zn diffusion ($p^+ \sim 10^{20}$ cm^{-3}) creates the conditions for formation of low resistance contacts. Table I presents the results of studying the behavior of the contact resistance at deposition of the metal layers Cr/Au, Cr/Ag, Cr/Ag(Mn), Ti/Pt/Au on p^+-GaSb surface.

Annealing	Composition			
	Cr/Au	Cr/Ag	Cr/Ag(Mn)	Ti/Pt/Au
As-deposited	$(3\text{-}5)\times10^{-6}$	$(3\text{-}6)\times10^{-5}$	$(8\text{-}9)\times10^{-6}$	$(4\text{-}6)\times10^{-6}$
H_2, 190^0C	$(7\text{-}9)\times10^{-6}$	$(2\text{-}3)\times10^{-5}$	$(3\text{-}4)\times10^{-5}$	$(8\text{-}9)\times10^{-6}$
H_2, 230^0C	$(1\text{-}2)\times10^{-5}$	$(2\text{-}3)\times10^{-5}$	$(2\text{-}3)\times10^{-5}$	-
N_2, 190^0C	$(8\text{-}9)\times10^{-6}$	$(4\text{-}5)\times10^{-5}$	$(7\text{-}9)\times10^{-6}$	$(5\text{-}7)\times10^{-6}$
N_2, 250^0C	$(4\text{-}5)\times10^{-6}$	-	-	$(1\text{-}3)\times10^{-6}$

Table I: Contact resistivity ($\Omega{\cdot}cm^2$) of various metallization systems on p^+-type GaSb.

The optimum annealing temperature range for the contacts considered is 190-250 ^0C. As follows from Table I, the contacts on the base of Cr/Au and Ti/Pt/Au are characterized by lower contact resistance. For this reasons, above compositions have been chosen by us for fabrication of contacts to *p*-GaSb.

Concerning to *n*-GaSb with a comparatively low doping level $(2\text{-}6){\cdot}10^{17}$ cm^{-3}, optimal for fabrication of high-efficient photocells, the following contact systems were investigated: Au(Ge)/Ni/Au, Au/Ni/Au and Au(Te)/Au.

As is seen from Fig. 5, the Au(Ge)/Ni/Au contacts are characterized by a minimum value of resistance at annealing temperatures of 220-260 ^0C. Figures 5 and 6 show the dependences of the resistance on annealing temperature for different ohmic contact compositions. As it is seen from Fig. 5 and 6, the contact resistance is lower for the case of higher doping level and achieves the values of $3{\cdot}10^{-6}$ $\Omega{\cdot}cm^2$ at $n = (1\text{-}3){\cdot}10^{18}$ cm^{-3}.

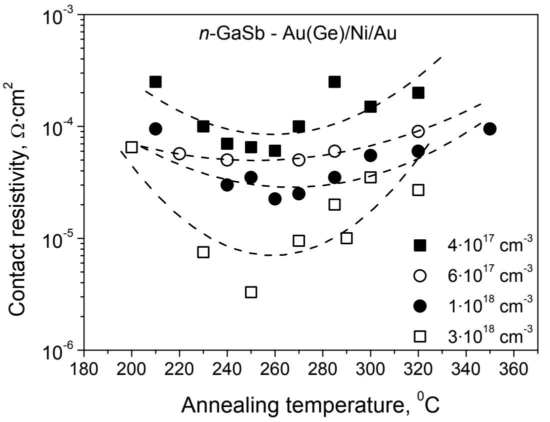

Figure 5: Dependence of the resistance of the Au(Ge)/Ni/Au ohmic contacts on the annealing temperature for different doping levels of the n-GaSb(Te) samples.

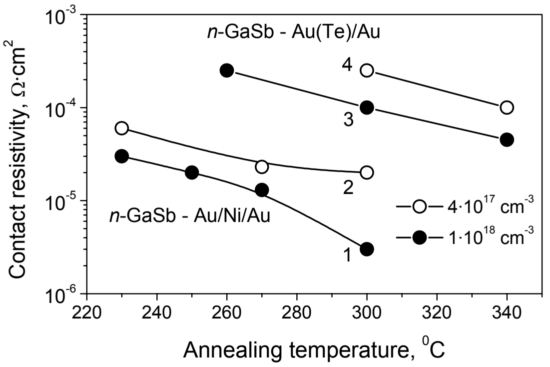

Figure 6: Dependence of the resistance of the Au/Ni/Au (curves 1, 2) and Au(Te)/Au (curves 3, 4) contacts on the annealing temperature for different doping levels of the n-GaSb(Te) samples.

The contact resistance for compositions Au/Ni/Au and Au(Te)/Au (Fig. 6) drops linearly at increasing the annealing temperature in the temperature range under study. However, its value for the Au/Ni/Au system is lower by an order of magnitude than that for the Au(Te)/Au system at the same annealing temperatures. A similar behavior was observed in [9].

4 GaSb SUBCELLS FOR MECHANICALLY STACKED TANDEM SOLAR CELLS

The results on optimum GaSb LPE growth conditions described above have been applied to development of the subcells for mechanically stacked tandem solar cells. To form p-n junctions the two-stage zinc diffusion process was used. The samples of 3.5x3.5 mm^2 in size had Cr/Au or Ti/Pt/Au front contact grid and Au(Ge)/Ni/Au back contact.

GaSb photocells of three types have been developed being a part of the mechanically stacked tandems: type 1 – with diffusion into the "bulk" n-GaSb wafer (doping level $n = (3\text{-}5)\cdot 10^{17}$ cm^{-3}) with a back epitaxial n^+-layer; type 2 – with diffusion into the GaSb epitaxial layer grown on a heavily doped ($n = 10^{18}$ cm^{-3}) GaSb substrate; type 3 – with diffusion into the "bulk" GaSb wafer ($n = (3\text{-}5)\cdot 10^{17}$ cm^{-3}) without both a back n^+-layer and a front epitaxial layer. Fig. 7 presents the efficiencies versus illumination level of the GaSb solar cells in mechanical stack with upper single-junction IR-transparent GaAs cell (GaAs doping level $n = 2\cdot 10^{17}$ cm^{-3}). As follows from Fig. 7, the cell with a back n^+-layer (curve 1), or that with front epitaxial layer grown on the heavily doped ($n = 10^{18}$ cm^{-3}) GaSb substrate (curve 2) has higher efficiency in comparison with the cells fabricated by diffusion directly into the GaSb wafers (curve 3). A lower fill factor in the cells based on "bulk" GaSb material (without a back n^+- layer or heavily doped substrate) being the reason for the efficiency drop is observed at the current density higher than 3 A/cm^2. Main reason for lower efficiencies was lower fill factor values especially for the case of current densities higher then 3 A/cm^2.

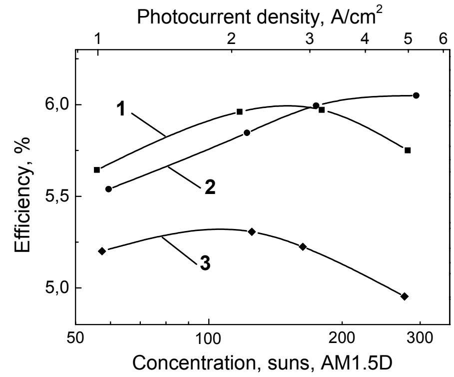

Figure 7: Conversion efficiency (AM 1.5D spectrum) vs. illumination density for the GaSb solar cells behind a top GaAs cell: curve 1 – the cell of type 1 (GaSb wafer, doping level of $n = 3\cdot 10^{17}$ cm^{-3}, back n^+- layer); curve 2 – the cell of type 2 (GaSb epitaxial layer on a heavily doped GaSb substrate); curve 3 – the cell of type 3 (bulk GaSb wafer, doping level of $n = 3\cdot 10^{17}$ cm^{-3}).

Fig. 8 presents photosensitivity spectra (AM1.5D) of the GaSb cells fabricated by diffusion process into the n-type epitaxial layers. The spectra were recorded in the following conditions: the cell as it is (curve 1); an infrared transparent single-junction GaAs cell is placed over (curve 2); a double-junction GaInP/GaInAs monolithic cell with GaAs substrate differing in thickness is placed over (curves 3, 4). Double layer ZnS/MgF_2 was used as an antireflecting coating.

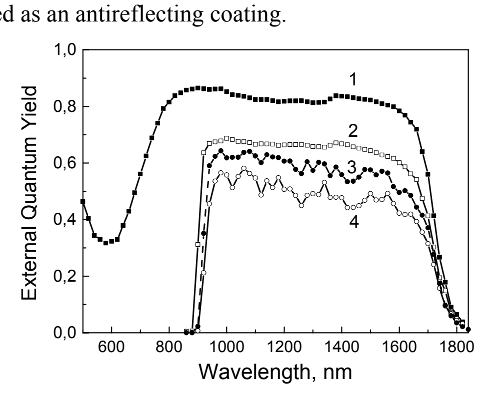

Figure 8: External quantum yield spectra of a GaSb solar cell: 1 – as it is, 2 – behind a GaAs SJ cell; 3, 4 – behind a top GaInP/GaInAs tandem cell. Curves 3 and 4 correspond to GaAs substrate thicknesses of 250 μm and 400 μm, respectively.

Spectral curves of Fig. 8 have been used for calculation of photocurrent densities, as well as conversion efficiencies of the cells in tandem mechanical stacks. Corresponding results are shown in Figure 9 vs. the sun concentration ratio (AM1.5D). As it is follows from Fig. 9, the maximum efficiency of sunlight conversion by GaSb cells achieves 6 % behind the GaAs top cell at concentration ratios of 100-200 suns, and 5.2 % behind a double-junction top GaInP/GaInAs cell at the GaAs substrate thickness of 250 μm.

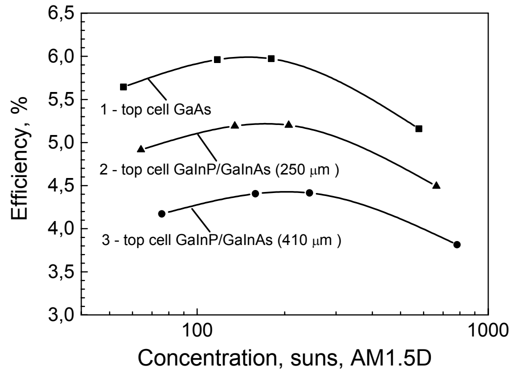

Figure 9: Efficiency of the GaSb - based solar cells: 1 – behind the GaAs top cell; 2, 3 - behind the GaInP/GaInAs top tandem cell.

5 GaSb AND InGaAsSb/GaSb TPV CELLS

Thermophotovoltaic cells based on GaSb and InGaAsSb/GaSb for conversion of radiation from tungsten emitters heated by concentrated sunlight [4, 5] have been fabricated. For this, a combination of LPE and zinc diffusion techniques has been used.

The 1 cm^2 in area GaSb cells were characterized by the following parameters: photocurrent density $J_{sc} = 4.5$ A/cm^2, open circuit voltage $V_{oc} = 0.49$ V and fill factor FF = 0.68 have been measured in GaSb cell in a PV module under illumination by solar powered tungsten emitter heated to the temperature of about 2000 K. Figures 10 and 11 present the values of above parameters for the developed TPV cells in dependence on tungsten emitter temperature. Efficiencies of 19 % in GaSb cells and 13 % in InGaAsSb cells have been estimated for described conditions.

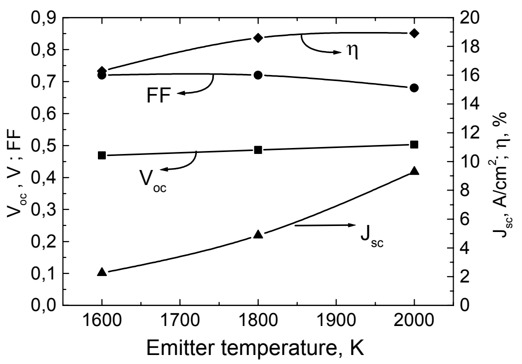

Figure 10: Dependences of the efficiency (η), fill factor (FF), open circuit voltage (V_{oc}) and short circuit current density (J_{sc}) for GaSb TPV cells on the tungsten emitter temperature.

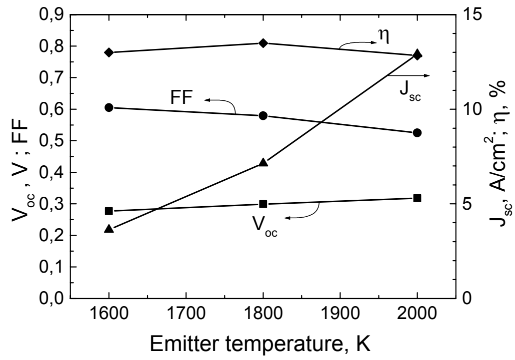

Figure 11: Dependences of efficiency (η), I-V characteristic fill factor (FF), open circuit voltage (V_{oc}) and short circuit current density (J_{sc}) for GaInAsSb TPV cells on the tungsten emitter temperature.

CONCLUSIONS

LPE epitaxial growth technique and contacting methodology have been developed in application to the bottom subcells in mechanically stacked solar cells and TPV converters. Efficiency of 19 % was obtained in GaSb cells and 13 % in InGaAsSb cells illuminated by a tungsten emitter heated up to 2000 K. Photocurrent density as high as 4.5 A/cm^2 was measured in a solar TPV module under illumination from a tungsten emitter.

ACKNOWLEDGEMENTS

Authors would like to express gratitude to N.H. Timoshina, A.V. Malevskaya, A.A. Usikova, V.I. Vasil'ev, A.N. Andreev, and M.G. Rastegaeva.

This work has been supported by the European Commission (FULLSPECTRUM Project SES6-CT-2003-502620) and Russian Foundation for the Basic Research (Grant № 03-02-17603).

REFERENCES

[1] L. Fraas, J. Avery, D. Scheiman, Proceedings 29th IEEE Photovoltaic Specialist Conference, (2002) 912.

[2] A.W. Bett, F. Dimroth, G. Stollwerck, O.V. Sulima, Appl. Phys. A69 (1999) 119.

[3] M.Z. Shvarts, V.M. Andreev, V.P. Khvostikov, V.R. Larionov, V.D. Rumyantsev, S.V. Sorokina, V.I. Vasil'ev, A.S. Vlasov, O.I. Chosta, Proceedings 5th European Space Power Conference, (1998) 527.

[4] V.M. Andreev, V.P. Khvostikov, V.D. Rumyantsev, P.Y. Gazaryan, A.S. Vlasov, N.A. Sadchikov, S.V. Sorokina, Y.M. Zadiranov, M.Z. Shvarts, Proceedings 20th European Photovoltaic Solar Energy Conference, (2005), (in this book).

[5] V.P. Khvostikov, V.D. Rumyantsev, P. Y. Gazaryan, S. V. Sorokina, M. Z. Shvarts, V. M. Andreev, Proceedings 31st IEEE Photovoltaic Specialists Conference and Exhibition, (2005), to be published.

[6] D. Martin, C. Algora, Semicond. Sci. Technol. 19 (2004) 1040.

[7] V.W.L. Chin, Solid-State Electronics, 38 (1995) 59.

[8] A.N. Andreev, M.G. Rastegaeva, V.P. Rastegaev, S.A. Reshanov, Semiconductors 32 (1998) 739.

[9] Ch. Heinz, Int. J. Electronics 54 (1983) 247.